NASA/TM–97–206271

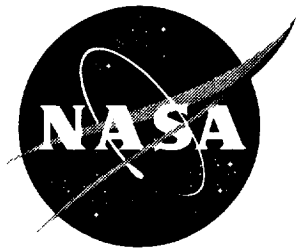

Equivalence of Fluctuation Splitting and Finite Volume for One-Dimensional Gas Dynamics

William A. Wood
Langley Research Center, Hampton, Virginia

National Aeronautics and
Space Administration

Langley Research Center
Hampton, Virginia 23681–2199

October 1997

Available from the following:

NASA Center for AeroSpace Information (CASI)
800 Elkridge Landing Road
Linthicum Heights, MD 21090–2934
(301) 621–0390

National Technical Information Service (NTIS)
5285 Port Royal Road
Springfield, VA 22161–2171
(703) 487–4650

Abstract

The equivalence of the discretized equations resulting from both fluctuation splitting and finite volume schemes is demonstrated in one dimension. Scalar equations are considered for advection, diffusion, and combined advection/diffusion. Analysis of systems is performed for the Euler and Navier-Stokes equations of gas dynamics. Non-uniform mesh-point distributions are included in the analyses.

Nomenclature

Geometric and independent variables

i	Computational indicie
L_{ref}	Non-dimensionalizing reference length
ℓ	Edge or element length
n	Normal vector
r	Distance vector
S	Generalized volume
t	Time
x	Physical coordinate, normalized by L_{ref}
Γ	Perimeter of control volume
Ω	Generalized integration volume

Dependent variables

$\mathbf{A}$	Flux Jacobian in conservative variables
$\mathcal{A}$	Flux Jacobian in auxiliary variables
a	Sound speed
c_p	Specific heat at constant pressure
c_v	Specific heat at constant volume
E	Total energy
e	Internal energy
$\mathbf{F}$	Flux function
$\mathbf{f}$	Numerical flux
H	Total enthalpy
h	Specific enthalpy
$\mathbf{M}$	Subsonic or supersonic matrix dissipation
P	Pressure
q	Heat flow
$\mathbf{R}$	Area-weighted residual
s	Entropy
T	Temperature
$\mathbf{U}$	Conserved variables
u, v, w	Cartesian velocities
$\mathbf{V}$	Primitive variables

$\mathbf{W}$	Auxiliary variables
$\mathbf{X}$	Matrix of right eigenvectors
$\mathcal{X}$	Right eigenvectors in auxiliary variables
$\mathbf{Z}$	Parameter vector
κ	Thermal conductivity
λ	Wavespeed
Λ	Eigenvalue matrix
ρ	Density
Φ	Artificial dissipation function
ϕ	Elemental fluctuation
$\breve{\phi}$	Fluctuation of auxiliary variables formulation
ϕ'	Elemental artificial dissipation
$\breve{\phi}'$	Artificial dissipation in auxiliary variables formulation
μ	Coefficient of viscosity
τ	Stress component

Auxiliary symbols

I	Identity matrix
M_ψ	Symmetric averaging function
p, q	Arguments of limiter
P_r	Prandtl number, $P_r(\text{air}) = 0.72$
$\Re$	Gas constant, $\Re(\text{air}) = 287$ J/(kg-K)
β	Limiter bound
ϵ	Eigenvalue limiting parameter
γ	Ratio of specific heats, $\gamma(\text{diatomic}) = 1.4$
υ	Finite element shape function
ψ	Limiter function

Operators

$\vec{\nabla}$	Gradient
∇^2	Laplacian, $\nabla^2 = \vec{\nabla} \cdot \vec{\nabla}$
Δ	Forward difference, $\Delta_i x = x_{i+1} - x_i$
∇	Backward difference, $\nabla_i x = x_i - x_{i-1}$
δ	Central difference, $\delta_i x = \frac{1}{2}(x_{i+1} - x_{i-1})$
δ^2	Second central difference, $\delta_i^2 x = \Delta\nabla_i x = \nabla\Delta_i x = x_{i+1} - 2x_i + x_{i-1}$

Acronyms

COE	Contributions from other elements
LHS	Left-hand side
RHS	Right-hand side

Subscripts

E	Element

L	Left-hand state
R	Right-hand state
U	Upwind
2U	Second-order upwind

Superscripts

i	Inviscid
v	Viscous

Overbars are used to represent cell-average values. Vector symbols indicate vectors spanning multiple spatial dimensions. Bold face is used for vectors and tensors of systems. Subscripts of variables is short-hand for differentiation. Hats denote unit vectors. Tildes denote Roe-averaged quantities.

Introduction

Finite volume flux-difference-split schemes, in particular the Roe scheme[1, 2] with a MUSCL[3] second-order extension, are well established for the solution of one-dimensional gas dynamics, with textbooks written on the subject[4]. The discretization of these schemes on general unstructured domains is well covered by Barth[5].

Fluctuation splitting concepts have been introduced for the solution of scalar advection problems in two dimensions[6, 7, 8], and are aligned with finite element concepts, as opposed to finite volumes. Notable work has been done by Sidilkover[9, 10, 11] to extend fluctuation splitting to the Euler system of equations for gas dynamics.

The current paper systematically establishes the equivalence of the discretized equations resulting from both fluctuation splitting and finite volume treatments of the Navier-Stokes equations in one dimension on non-uniform meshes. The fluctuation splitting development is performed as quadrature over discrete elements, in contrast to the usual treatment which resorts to a flux formula *via* the divergence theorem. Scalar equations are considered first, covering advection, diffusion, and combined advection/diffusion. Then the Euler system is considered, equating Roe's wave-decomposition procedure with Sidilkover's modified auxiliary equations approach. Discretization of viscous and conductive terms completes the analysis for the Navier-Stokes equations.

The equivalence of fluctuation splitting and finite volume in one dimension serves as a prelude to multidimensional analysis, where the methods differ. Results by Sidilkover[12] suggest there may be definite advantages to fluctuation splitting over finite volume for the multidimensional Euler equations. However, other researchers[13] have not found an advantage in fluctuation splitting, though their treatment of the Euler equations differs significantly from that of Sidilkover.

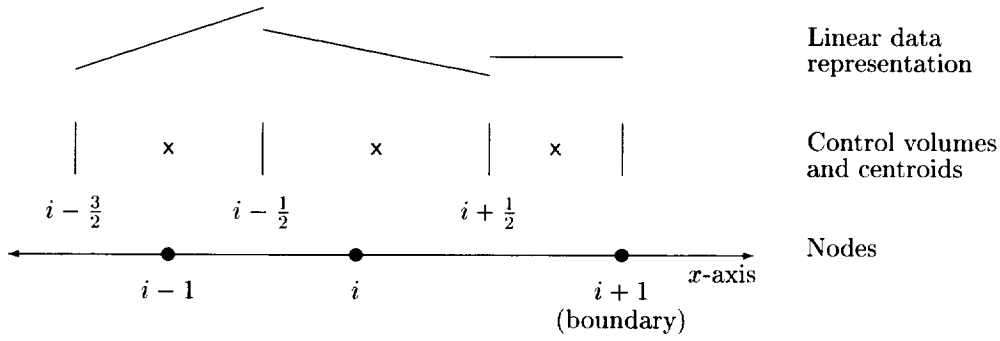

Figure 1: One-dimensional finite volume domain.

Domain

In one dimension the domain considered is a discretization of the x-axis, either with uniform or non-uniform spacing between grid nodes, which are indexed by i. Dependent variables are stored as discreet nodal values.

In a finite volume context a median-dual control volume is constructed about each node by defining a cell face halfway between adjacent nodes. This convention is depicted in Figure 1, with the cell faces referred to as the $\pm\frac{1}{2}$ points. In the illustrative case of Figure 1, the $i+1$ node is a boundary point, and the corresponding cell extends only from $i+\frac{1}{2}$ to $i+1$. The generalized volume of the control cell is,

$$S_i = x_{i+\frac{1}{2}} - x_{i-\frac{1}{2}} = \frac{x_{i+1}+x_i}{2} - \frac{x_i+x_{i-1}}{2} = \frac{x_{i+1}-x_{i-1}}{2} = \delta_i x \qquad (1)$$

There is a one-to-one correspondence between the nodes and control volumes.

Notice that for the nodal distribution depicted, which has non-uniform spacing, the cell centroids, denoted by x in Figure 1, do not coincide with the nodes. Barth[5] states that nodal storage in this case, referred to as mass lumping in a finite element context, only alters the time accuracy of finite volume schemes, and not the steady state solutions.

Notice also the piecewise-linear representation of data in the finite volume context. Discontinuous jumps in the dependent data are allowed at cell faces.

Figure 2 depicts the discretization of the domain for the fluctuation splitting approach. The data is now continuous and piecewise linear over elements defined by the nodes. The centroids of the fluctuation splitting elements are at the same locations as the faces of the finite volume cells. No special definition of a boundary cell is required. The length of an element is,

$$\ell_{i,i+1} = x_{i+1} - x_i = \Delta_i x \qquad (2)$$

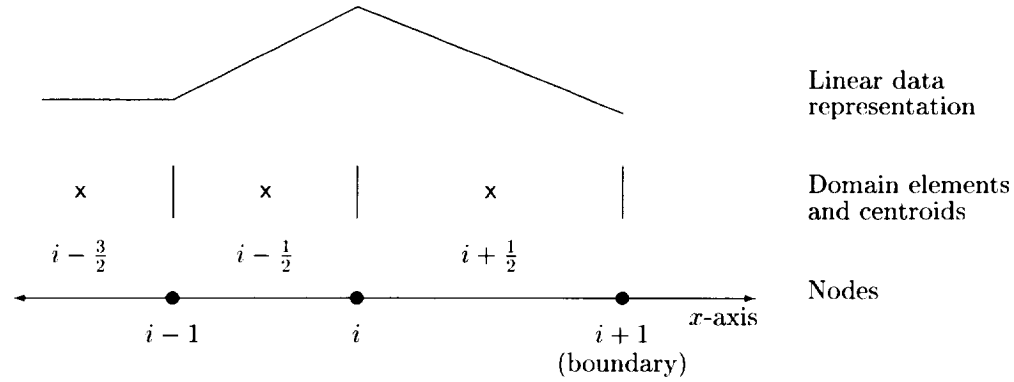

Figure 2: One-dimensional fluctuation splitting domain.

There are one fewer elements than nodes, and each element is associated with two nodes. Correspondingly, each interior node is associated with two elements, while each boundary node is associated with only one element.

Scalar Advection

A hyperbolic conservation law takes the form,

$$\mathbf{U}_t + \vec{\nabla} \cdot \vec{\mathbf{F}} = 0 \tag{3}$$

where $\mathbf{U}$ is the vector of conserved variables and $\vec{\mathbf{F}}$ is the flux of these variables. Following Godunov[14], Eqn. 3 can be evaluated in an integral sense,

$$\int_\Omega \mathbf{U}_t \, d\Omega = -\int_\Omega \vec{\nabla} \cdot \vec{\mathbf{F}} \, d\Omega \tag{4}$$

If the control volume, Ω, is fixed in time, then,

$$\int_\Omega \mathbf{U}_t \, d\Omega = S_\Omega \bar{\mathbf{U}}_t \tag{5}$$

where the overbar indicates some cell-average value. Using the divergence theorem the flux term can be evaluated as,

$$\int_\Omega \vec{\nabla} \cdot \vec{\mathbf{F}} \, d\Omega = \oint_\Gamma \vec{\mathbf{F}} \cdot \hat{n} \, d\Gamma \tag{6}$$

where $\hat{n}$ is the outward unit normal to the control volume boundary, Γ.

The one-dimensional scalar advection problem is obtained from Eqn. 3 as,

$$u_t + F_x = 0 \tag{7}$$

which can be written for a control cell as,

$$S_\Omega \bar{u}_t = -\int_\Omega F_x \, d\Omega = F_{left\ face} - F_{right\ face} \tag{8}$$

Linear Advection

Linear advection is obtained from Eqn. 7 by choosing $F = \lambda u$. The advection speed, λ, is taken to be constant.

Finite Volume

Equation 8 is expressed for the finite volume about node i with mass lumping to the node as,

$$S_i u_{i_t} = F_{i-\frac{1}{2}} - F_{i+\frac{1}{2}} \cong f_{i-\frac{1}{2}} - f_{i+\frac{1}{2}} = R_i \tag{9}$$

where the numerical flux, f, is a difference expression approximating the exact flux function, F. Choosing,

$$f_{i+\frac{1}{2}} = \frac{F_i + F_{i+1}}{2} \tag{10}$$

results in a second-order central difference scheme,

$$R_i = -\delta_i F \tag{11}$$

The first-order upwind CIR[15] scheme is obtained by the choice,

$$f_{i+\frac{1}{2}} = \frac{\lambda + |\lambda|}{2} u_i + \frac{\lambda - |\lambda|}{2} u_{i+1} \tag{12}$$

$$= \frac{F_i + F_{i+1}}{2} - \frac{|\lambda|}{2} \Delta_i u \tag{13}$$

giving,

$$R_i = -\delta_i F + \frac{|\lambda|}{2} \delta_i^2 u \tag{14}$$

The first-order upwind is then seen to be the same as a central distribution plus an artificial dissipation term,

$$\Phi_U = \frac{|\lambda|}{2} \delta_i^2 u \tag{15}$$

Second-order upwind is constructed following the MUSCL concept of van Leer[3], where a linear reconstruction is performed on each finite volume. The numerical flux of Eqn. 12 is modified to be,

$$f_{i+\frac{1}{2}} = \frac{\lambda + |\lambda|}{2} u_L + \frac{\lambda - |\lambda|}{2} u_R \tag{16}$$

where u_{L} is the reconstructed conserved variable on the left side of the cell face and u_{R} is the reconstructed variable on the right side of the cell face. Following Barth[5], a limited reconstruction is performed on each cell as,

$$u_{face} = u_i + \psi_i (\vec{\nabla} u)_i \cdot \vec{r}_{face} \tag{17}$$

The gradient is evaluated as a central difference,

$$(\vec{\nabla} u)_i = \frac{\delta_i u}{S_i} \tag{18}$$

The limiter function, ψ, is employed to provide monotonicity of the solution, based upon positivity arguments. The limiter takes the form,

$$\psi\left(\frac{p}{q}\right)$$

where,

$$p = \frac{u_{i\pm1} - u_i}{2}, \quad q = (\vec{\nabla} u)_i \cdot \vec{r}_{i\pm\frac{1}{2}}$$

The more restrictive of the $\pm$ choices is used for ψ. Some popular limiters are presented in the appendix.

The discrete numerical flux (Eqn. 16) expands to,

$$\begin{aligned} f_{i+\frac{1}{2}} = & \frac{\lambda + |\lambda|}{2}\left(u_i + \psi_i \frac{\ell_{i,i+1}}{2S_i}\delta_i u\right) + \frac{\lambda - |\lambda|}{2}\left(u_{i+1} - \psi_{i+1}\frac{\ell_{i,i+1}}{2S_{i+1}}\delta_{i+1} u\right) \\ = & \frac{F_i + F_{i+1}}{2} - \frac{|\lambda|}{2}\Delta_i u + \frac{\ell_{i,i+1}}{4}\left(\frac{\psi_i}{S_i}\delta_i(F+|\lambda|u) - \frac{\psi_{i+1}}{S_{i+1}}\delta_{i+1}(F-|\lambda|u)\right) \end{aligned} \tag{19}$$

leading to,

$$R_i = -\delta_i F + \Phi_{\mathsf{U}} + R_{2\mathsf{U}} \tag{20}$$

where the second-order correction is,

$$\begin{aligned} R_{2\mathsf{U}} = & \frac{\ell_{i-1,i}}{4}\left(\frac{\psi_{i-1}}{S_{i-1}}\delta_{i-1}(F+|\lambda|u) - \frac{\psi_i}{S_i}\delta_i(F-|\lambda|u)\right) \\ - & \frac{\ell_{i,i+1}}{4}\left(\frac{\psi_i}{S_i}\delta_i(F+|\lambda|u) - \frac{\psi_{i+1}}{S_{i+1}}\delta_{i+1}(F-|\lambda|u)\right) \end{aligned} \tag{21}$$

The residual (Eqn. 20) can be rearranged as,

$$\begin{aligned} R_i = & -\delta_i F - \frac{1}{8}\left[\ell_{i-1,i}\frac{\psi_{i-1}}{S_{i-1}}F_{i-2} - 2\psi_i F_{i-1} + \left(\ell_{i,i+1}\frac{\psi_{i+1}}{S_{i+1}} - \ell_{i-1,i}\frac{\psi_{i-1}}{S_{i-1}}\right)F_i\right. \\ & \left. + 2\psi_i F_{i+1} - \ell_{i,i+1}\frac{\psi_{i+1}}{S_{i+1}}F_{i+2}\right] + \Phi_{2\mathsf{U}} \end{aligned} \tag{22}$$

where the artificial dissipation is now,

$$\begin{aligned}\Phi_{2U} &= \Phi_U + \frac{|\lambda|}{8}\left[-\ell_{i-1,i}\frac{\psi_{i-1}}{S_{i-1}}u_{i-2} + \frac{\psi_i}{S_i}\left(\ell_{i,i+1} - \ell_{i-1,i}\right)u_{i-1}\right. \\ &+ \left(\ell_{i-1,i}\frac{\psi_{i-1}}{S_{i-1}} + \ell_{i,i+1}\frac{\psi_{i+1}}{S_{i+1}}\right)u_i - \frac{\psi_i}{S_i}\left(\ell_{i,i+1} - \ell_{i-1,i}\right)u_{i+1} \\ &- \left.\ell_{i,i+1}\frac{\psi_{i+1}}{S_{i+1}}u_{i+2}\right] \end{aligned} \tag{23}$$

On a uniform grid and without limiting, the second-order residual (Eqn. 22) reduces to a low-truncation-error central difference minus fourth-order dissipation,

$$R_i = \frac{1}{8}\left(-F_{i-2} + 6F_{i-1} - 6F_{i+1} + F_{i+2}\right) + \frac{|\lambda|}{8}\left(-u_{i-2} + 4u_{i-1} - 6u_i + 4u_{i+1} - u_{i+2}\right) \tag{24}$$

Fluctuation splitting

In the fluctuation splitting framework Eqn. 8 is evaluated over each domain element, without recourse to the divergence theorem. The element fluctuation is defined as,

$$S_\Omega \bar{u}_t = \phi_E = -\int_\Omega F_x \, d\Omega \tag{25}$$

Assuming piecewise linear data, the fluctuation for the cell bounded by x_i and x_{i+1} is evaluated as,

$$\phi_{i,i+1} = -\lambda \int_{x_i}^{x_{i+1}} u_x \, d\ell = -\ell_{i,i+1}\,\lambda \frac{\Delta_i u}{\Delta_i x} = -\Delta_i F \tag{26}$$

The elemental update, the LHS of Eqn. 25, is formed as,

$$S_\Omega \bar{u}_t = \ell_{i,i+1}\left(\frac{u_i + u_{i+1}}{2}\right)_t = \frac{\ell_{i,i+1}}{2}(u_{i_t} + u_{i+1_t}) = \phi_{i,i+1} \tag{27}$$

Partitioning the fluctuation into halves and distributing equally to the nodes yields the elemental update formula,

$$\frac{\ell_{i,i+1}}{2}u_{i_t} = \frac{\phi_{i,i+1}}{2}, \quad \frac{\ell_{i,i+1}}{2}u_{i+1_t} = \frac{\phi_{i,i+1}}{2} \tag{28}$$

Assembling all the elemental contributions to the nodal updates, it is clear each interior node will receive fluctuation signals from the elements adjacent to the left and right. The nodal update is formed as the sum of these fluctuation contributions,

$$\frac{\ell_{i-1,i}}{2}u_{i_t} + \frac{\ell_{i,i+1}}{2}u_{i_t} = \frac{\ell_{i-1,i} + \ell_{i,i+1}}{2}u_{i_t} = S_i u_{i_t} = \frac{\phi_{i-1,i}}{2} + \frac{\phi_{i,i+1}}{2} \tag{29}$$

or,

$$S_i u_{i_t} = \frac{\phi_{i-1,i} + \phi_{i,i+1}}{2} \tag{30}$$

A popular nomenclature convention for Eqns. 28 and 30 is to describe the elemental distribution formula as,

$$S_i u_{i_t} \leftarrow \frac{\phi_{i,i+1}}{2} + \text{COE}, \quad S_{i+1} u_{i+1_t} \leftarrow \frac{\phi_{i,i+1}}{2} + \text{COE} \tag{31}$$

where COE indicates a sum of similar contributions from other elements joining at that node.

Expanding the nodal update formula (Eqn. 30),

$$S_i u_{i_t} = \frac{-\nabla_i F - \Delta_i F}{2} = -\delta_i F \tag{32}$$

which is the identical central discretization as for finite volume (Eqn. 11).

An upwind scheme can be constructed by introducing artificial dissipation in order to redistribute the fluctuation,

$$\phi'_{\mathsf{E}} = \text{sign}(\lambda)\phi_{\mathsf{E}} \tag{33}$$

The upwind distribution formula becomes,

$$\begin{aligned} S_i u_{i_t} &\leftarrow \frac{\phi_{\mathsf{E}} - \phi'_{\mathsf{E}}}{2} + \text{COE} = \frac{\phi_{i,i+1}(1 - \text{sign}(\lambda))}{2} + \text{COE} \\ S_{i+1} u_{i+1_t} &\leftarrow \frac{\phi_{\mathsf{E}} + \phi'_{\mathsf{E}}}{2} + \text{COE} = \frac{\phi_{i,i+1}(1 + \text{sign}(\lambda))}{2} + \text{COE} \end{aligned} \tag{34}$$

Using the fluctuation definition (Eqn. 26) the nodal update is obtained as,

$$S_i u_{i_t} = -\frac{(\lambda + |\lambda|)\nabla_i u}{2} - \frac{(\lambda - |\lambda|)\Delta_i u}{2} = -\delta_i F + \frac{|\lambda|}{2}\delta_i^2 u \tag{35}$$

which is identical to the first-order upwind discretization for finite volume (Eqn. 14).

A second-order scheme is easily obtained by adding the exact same finite volume correction, $R_{2\mathsf{U}}$ (Eqn. 21), to the nodal update formula (Eqn. 35).

Non-linear Advection

Non-linear advection is obtained from Eqn. 7 by choosing the flux to be,

$$F = \frac{u^2}{2} \tag{36}$$

Define the Jacobian of the flux,

$$A = F_u \tag{37}$$

so that,

$$F_x = \frac{\partial F}{\partial x} = \frac{\partial F}{\partial u}\frac{\partial u}{\partial x} = F_u u_x = A u_x$$

Equation 7 may be rearranged in non-conservation form,

$$u_t + F_x = u_t + A u_x = 0 \tag{38}$$

Finite volume

Following Roe[1], the analog to the numerical flux of Eqn. 16 becomes,

$$\begin{aligned} f_{i+\frac{1}{2}} &= \frac{A_{\mathsf{L}} + |\tilde{A}|_{i+\frac{1}{2}}}{2} u_{\mathsf{L}} + \frac{A_{\mathsf{R}} - |\tilde{A}|_{i+\frac{1}{2}}}{2} u_{\mathsf{R}} \\ &= \frac{F_{\mathsf{L}} + F_{\mathsf{R}}}{2} - \frac{|\tilde{A}|_{i+\frac{1}{2}}}{2}(u_{\mathsf{R}} - u_{\mathsf{L}}) \end{aligned} \tag{39}$$

where $\tilde{A}$ is the conservative linearization, which in this case is,

$$\tilde{A}_{i+\frac{1}{2}} = \frac{u_{\mathsf{L}} + u_{\mathsf{R}}}{2} \tag{40}$$

A first-order upwind scheme is obtained using piecewise-constant data, $u_{\mathsf{L}} = u_i$, and $u_{\mathsf{R}} = u_{i+1}$. A second-order upwind scheme is constructed using the linear reconstruction of Eqn. 17. The first-order residual may be written explicitly as,

$$R_i = -\delta_i F + \frac{|\tilde{A}|_{i+\frac{1}{2}}}{2} \Delta_i u - \frac{|\tilde{A}|_{i-\frac{1}{2}}}{2} \nabla_i u \tag{41}$$

Fluctuation splitting

The elemental fluctuation is

$$\phi_{\mathsf{E}} = -\int_{\Omega} F_x \, d\Omega = -\int_{\Omega} A u_x \, d\Omega \tag{42}$$

Assuming piecewise-linear data Eqn. 42 becomes,

$$\phi_{\mathsf{E}} = -\tilde{A}_{i+\frac{1}{2}} \Delta_i u = -\Delta_i F \tag{43}$$

An upwind scheme is created by introducing the artificial dissipation,

$$\phi'_{\mathsf{E}} = \text{sign}(\tilde{A}_{i+\frac{1}{2}}) \phi_{\mathsf{E}} = -|\tilde{A}|_{i+\frac{1}{2}} \Delta_i u \tag{44}$$

The distribution formula remains,

$$\begin{aligned} S_i u_{i_t} &\leftarrow \frac{\phi_{\mathsf{E}} - \phi'_{\mathsf{E}}}{2} + \text{COE} \\ S_{i+1} u_{i+1_t} &\leftarrow \frac{\phi_{\mathsf{E}} + \phi'_{\mathsf{E}}}{2} + \text{COE} \end{aligned} \tag{45}$$

The nodal update is,

$$\begin{aligned} S_i u_{i_t} &= \frac{\phi_{i-1,i} + \phi'_{i-1,i}}{2} + \frac{\phi_{i,i+1} - \phi'_{i,i+1}}{2} \\ &= -\frac{\nabla_i F}{2} - \frac{|\tilde{A}|_{i-\frac{1}{2}}}{2} \nabla_i u - \frac{\Delta_i F}{2} + \frac{|\tilde{A}|_{i+\frac{1}{2}}}{2} \Delta_i u \\ &= -\delta_i F - \frac{|\tilde{A}|_{i-\frac{1}{2}}}{2} \nabla_i u + \frac{|\tilde{A}|_{i+\frac{1}{2}}}{2} \Delta_i u \end{aligned} \tag{46}$$

This is the identical update formula as for finite volume (Eqn. 41).

Expansion shocks

The discretization of Roe's scheme allows for unphysical expansion shocks that violate the entropy condition. Harten and Hyman[16] proposed a commonly used method for perturbing the wavespeeds such that entropy is satisfied and expansion shocks are prevented. The correction is applied to any wavespeed that can go to zero at a sonic point and takes the form,

$$|\tilde{\lambda}|_{i+\frac{1}{2}} \leftarrow \max\left[|\tilde{\lambda}|_{i+\frac{1}{2}}, \quad \frac{1}{2}\left(\frac{\tilde{\lambda}^2_{i+\frac{1}{2}}}{\epsilon} + \epsilon\right)\right] \tag{47}$$

where the perturbation scale is,

$$\epsilon = \max\left[0, \quad (\tilde{\lambda}_{i+\frac{1}{2}} - \lambda_i), \quad (\lambda_{i+1} - \tilde{\lambda}_{i+\frac{1}{2}})\right] \tag{48}$$

Scalar Advection/Diffusion

The governing equation for scalar advection/diffusion problems in one-dimension is,

$$u_t + F_x = (\mu u_x)_x \tag{49}$$

Heat Equation

Modeling of the viscous RHS in Eqn. 49 begins with a consideration of the heat equation,

$$u_t = (\mu u_x)_x \tag{50}$$

In the finite volume framework one approach to discretizing the viscous term is to construct a viscous flux, so that the nodal update becomes,

$$S_i u_{i_t} = (\bar{\mu} u_x)_{i+\frac{1}{2}} - (\bar{\mu} u_x)_{i-\frac{1}{2}} \tag{51}$$

where,

$$(\bar{\mu} u_x)_{i+\frac{1}{2}} = \bar{\mu}_{i+\frac{1}{2}}\left[\frac{(\vec{\nabla} u)_i + (\vec{\nabla} u)_{i+1}}{2}\right] \tag{52}$$

with the gradients $\vec{\nabla} u$ defined by Eqn. 18. This approach leads to a five-point stencil.

An alternative is to use a finite element discretization, which results in a three-point stencil. This approach is adopted both by Barth[5] and Anderson and Bonhaus[17] in a finite volume context and by Tomaich[18] in a fluctuation splitting context.

A Galerkin finite element discretization, using mass lumping to the nodes, is constructed on the fluctuation splitting domain by integrating with the aid

of the finite element linear shape function v (see Bickford §4.2.2[19] or Bathe §7.2[20]),

$$S_i u_{i_t} = \int_\Omega v_i (\mu u_x)_x \, d\Omega \tag{53}$$

Integrating by parts,

$$S_i u_{i_t} = v_i (\mu u_x)|_{i-1}^{i+1} - \int_\Omega (v_i)_x (\mu u_x) \, d\Omega \tag{54}$$

The shape function is the linear tent function, and is equal to zero at $x_{i\pm1}$, eliminating the first RHS term of Eqn. 54. The remaining term is integrated over each element connecting at node i,

$$S_i u_{i_t} = -\sum_E \int_E v_x u_x \mu \, d\Omega \tag{55}$$

The dependent variable and shape function gradients are constant over the element, and taking the element-average viscosity coefficient the elemental contributions are,

$$\begin{aligned} S_i u_{i_t} &\leftarrow \frac{\Delta_i u}{\ell_{i,i+1}} \bar{\mu}_{i+\frac{1}{2}} + \text{COE} \\ S_{i+1} u_{i+1_t} &\leftarrow -\frac{\Delta_i u}{\ell_{i,i+1}} \bar{\mu}_{i+\frac{1}{2}} + \text{COE} \end{aligned} \tag{56}$$

The nodal update is written,

$$S_i u_{i_t} = \frac{\Delta_i u}{\ell_{i,i+1}} \bar{\mu}_{i+\frac{1}{2}} - \frac{\nabla_i u}{\ell_{i-1,i}} \bar{\mu}_{i-\frac{1}{2}} \tag{57}$$

Combined Advection and Diffusion

The combined effects of advection and diffusion in the governing equation (Eqn. 49) are treated by discretizing the advection terms as discussed in the Scalar Advection section and adding the discretization of the diffusion terms from the Heat Equation subsection. Recall, however, that the upwind advection discretization includes artificial dissipation, which can mask the physical dissipation.

The best approach for solving discretized advection/diffusion problems, as suggested by Barth[21], is to include the maximum of either the physical diffusion term, as defined by Eqn. 52 or Eqn. 56, or the artificial dissipation, the second term of Eqn. 39 for finite volume or $\frac{\phi_E'}{2}$ in Eqn. 44 for fluctuation splitting.

Systems

A hyperbolic conservation law for systems (Eqn. 3) is written in one dimension as,

$$\mathbf{U}_t + \mathbf{F}_x = 0 \tag{58}$$

A decomposition of the flux function is sought such that the system can be expressed as a decoupled set of advection/diffusion equations.

Euler Equations

The one-dimensional Euler equations[22] for perfect gases, suitable for simulating non-reacting, low-Knudson-number shock-tube flows, are written as a conservation law (Eqn. 58) with,

$$\mathbf{U} = \left\{ \begin{array}{c} \rho \\ \rho u \\ \rho E \end{array} \right\} \tag{59}$$

$$\mathbf{F} = \left\{ \begin{array}{c} \rho u \\ \rho u + P \\ \rho u H \end{array} \right\} \tag{60}$$

The Euler equations have a form similar to the non-linear advection problem.

The total energy and enthalpy are obtained from the internal energy and enthalpy,

$$E = e + \frac{u^2}{2} \qquad H = h + \frac{u^2}{2}$$

The energy and enthalpy are related as,

$$h = e + \frac{p}{\rho}$$

And the equation of state is,

$$P = \rho e(\gamma - 1) \tag{61}$$

Finite volume

The numerical flux remains as in Eqn. 39,

$$\mathbf{f}_{i+\frac{1}{2}} = \frac{\mathbf{F}_\mathsf{L} + \mathbf{F}_\mathsf{R}}{2} - \frac{|\tilde{\mathbf{A}}|_{i+\frac{1}{2}}}{2}(\mathbf{U}_\mathsf{R} - \mathbf{U}_\mathsf{L}) \tag{62}$$

Roe[1, 2] constructs the conservative linearization for the $|\tilde{\mathbf{A}}|_{i+\frac{1}{2}}$ matrix by introducing the parameter vector,

$$\mathbf{Z} = \sqrt{\rho} \left\{ \begin{array}{c} 1 \\ u \\ H \end{array} \right\} \tag{63}$$

The $i + \frac{1}{2}$ state is taken to be a linear average of the parameter vector,

$$\bar{\mathbf{Z}}_{i+\frac{1}{2}} = \frac{\mathbf{Z}_\mathsf{L} + \mathbf{Z}_\mathsf{R}}{2}$$

Taking the velocity and total enthalpy from the parameter vector,

$$\tilde{u} = \frac{\bar{z}_2}{\bar{z}_1} \qquad \tilde{H} = \frac{\bar{z}_3}{\bar{z}_1} \tag{64}$$

and defining the Roe-density,

$$\tilde{\rho} = \sqrt{\rho_{\mathsf{L}}\rho_{\mathsf{R}}} \tag{65}$$

the Jacobian matrix is formed as,

$$|\tilde{\mathbf{A}}| = \tilde{\mathbf{X}}|\tilde{\mathbf{\Lambda}}|\tilde{\mathbf{X}}^{-1} \tag{66}$$

The eigenvalues are,

$$\mathbf{\Lambda} = \mathrm{diag}(u,\ u+a,\ u-a) \tag{67}$$

The right eigenvectors are,

$$\mathbf{X}^{(1)} = \begin{Bmatrix} 1 \\ u \\ \frac{u^2}{2} \end{Bmatrix} \quad \mathbf{X}^{(2)} = \begin{Bmatrix} 1 \\ u+a \\ H+ua \end{Bmatrix} \quad \mathbf{X}^{(3)} = \begin{Bmatrix} 1 \\ u-a \\ H-ua \end{Bmatrix} \tag{68}$$

The product $\tilde{\mathbf{X}}^{-1}(\mathbf{U}_{\mathsf{R}} - \mathbf{U}_{\mathsf{L}})$ is evaluated *via* the characteristic variables,

$$\tilde{\mathbf{X}}^{-1}(\mathbf{U}_{\mathsf{R}} - \mathbf{U}_{\mathsf{L}}) = \tilde{\mathbf{X}}^{-1}d\mathbf{U} = \frac{1}{2\tilde{a}^2}\begin{Bmatrix} 2\tilde{a}^2 d\rho - 2dP \\ dP + \tilde{\rho}\tilde{a}du \\ dP - \tilde{\rho}\tilde{a}du \end{Bmatrix} \tag{69}$$

The sound speed is,

$$a^2 = \frac{\gamma P}{\rho} = \gamma(\gamma-1)e = (\gamma-1)h = (\gamma-1)(H - \frac{u^2}{2}) \tag{70}$$

Also note the grouping $\tilde{\rho}du$ can be constructed as,

$$\tilde{\rho}du = \bar{z}_1 dz_2 - \bar{z}_2 dz_1 \tag{71}$$

As for the scalar case, first-order spatial accuracy is obtained by taking the right state to be $i+1$ and the left state at i. Higher-order accuracy is obtained using gradient reconstruction (Eqn. 17) applied either to each of the conserved variables (Eqn.59) or each of the primitive variables, which are,

$$\mathbf{V} = \begin{Bmatrix} \rho \\ u \\ P \end{Bmatrix} \tag{72}$$

The nodal update is still formed as in Eqn. 9. The residual remains as expressed in Eqn. 41, but for systems rather than scalar quantities.

Fluctuation splitting

The Euler flux (Eqn. 60) can be written in terms of the parameter vector,

$$\mathbf{F} = \begin{Bmatrix} Z_1 Z_2 \\ \frac{\gamma-1}{\gamma} Z_1 Z_3 + \frac{\gamma+1}{2\gamma} Z_2^2 \\ Z_2 Z_3 \end{Bmatrix} \tag{73}$$

Further, the derivative of the flux is,

$$d\mathbf{F} = \begin{bmatrix} Z_2 & Z_1 & 0 \\ \frac{\gamma-1}{\gamma} Z_3 & \frac{\gamma+1}{\gamma} Z_2 & \frac{\gamma-1}{\gamma} Z_1 \\ 0 & Z_3 & Z_2 \end{bmatrix} d\mathbf{Z} \tag{74}$$

By assuming a linear variation of the parameter vector on each element, the fluctuation is obtained from Eqn. 42 as,

$$\phi_{\mathsf{E}} = -\int_{\Omega} \mathbf{F}_x \, d\Omega = -\int_{\Omega} \mathbf{F}_Z \mathbf{Z}_x \, d\Omega = -\bar{\mathbf{F}}_Z \Delta_i \mathbf{Z} \tag{75}$$

Deconinck *et al*[23] show,

$$\bar{\mathbf{F}}_Z \Delta_i \mathbf{Z} = \tilde{\mathbf{A}} \Delta_i \mathbf{U} = \Delta_i \mathbf{F} \tag{76}$$

when the Roe-averaged forms (Eqns. 64 and 65) are used to obtain $\tilde{\mathbf{A}}$.

An upwind scheme is constructed by adding the artificial dissipation,

$$\phi'_{\mathsf{E}} = -|\tilde{\mathbf{A}}|_{i+\frac{1}{2}} \Delta_i \mathbf{U} \tag{77}$$

where $|\tilde{\mathbf{A}}|$ is defined in Eqn. 66. Employing the same distribution formula as for the scalar advection (Eqn. 45) leads to an update formula analogous to Eqn. 46, showing the equivalence between finite volume and fluctuation splitting for the one-dimensional Euler equations.

Before ending the fluctuation splitting discussion, it is desired to frame the artificial dissipation in the form,

$$\phi'_{\mathsf{E}} = \text{sign}(\tilde{\mathbf{A}}_{i+\frac{1}{2}}) \phi_{\mathsf{E}} \tag{78}$$

The difficulty lies in defining the matrix $\text{sign}(\tilde{\mathbf{A}})$. One expression equates Eqns. 66, 75, 76, 77, and 78 to form,

$$\begin{aligned} \text{sign}(\tilde{\mathbf{A}})\tilde{\mathbf{A}} &= |\tilde{\mathbf{A}}| = \tilde{\mathbf{X}}|\tilde{\mathbf{\Lambda}}|\tilde{\mathbf{X}}^{-1} \\ \text{sign}(\tilde{\mathbf{A}}) &= \tilde{\mathbf{X}}|\tilde{\mathbf{\Lambda}}|\tilde{\mathbf{X}}^{-1}\tilde{\mathbf{A}}^{-1} = \tilde{\mathbf{X}}|\tilde{\mathbf{\Lambda}}|\tilde{\mathbf{\Lambda}}^{-1}\tilde{\mathbf{X}}^{-1} \end{aligned} \tag{79}$$

Sidilkover[9] offers an alternative to brute force matrix multiplications for evaluating Eqn. 79. Introducing the auxiliary variables, $\mathbf{W}$, defined by the transformation,

$$d\mathbf{U} = \mathbf{U}_W d\mathbf{W} \tag{80}$$

where,

$$d\mathbf{W} = \left\{ \begin{array}{c} ds \\ \tilde{\rho} du \\ dP \end{array} \right\} \tag{81}$$

with the entropy defined as,

$$ds = d\rho - \frac{dP}{a^2} \tag{82}$$

The Jacobian of the transformation is,

$$\mathbf{U}_W = \left[\begin{array}{ccc} 1 & 0 & \frac{1}{a^2} \\ u & 1 & \frac{u}{a^2} \\ \frac{u^2}{2} & u & \frac{1}{\gamma - 1} + \frac{u^2}{2a^2} \end{array} \right] \tag{83}$$

and its inverse is,

$$\mathbf{U}_W^{-1} = \left[\begin{array}{ccc} 1 - (\gamma - 1)\frac{u^2}{2a^2} & (\gamma - 1)\frac{u}{a^2} & -(\gamma - 1)\frac{1}{a^2} \\ -u & 1 & 0 \\ (\gamma - 1)\frac{u^2}{2} & -(\gamma - 1)u & \gamma - 1 \end{array} \right] \tag{84}$$

The element fluctuation (Eqn. 75) can be reworked,

$$\phi_{\mathsf{E}} = -\tilde{\mathbf{A}} \Delta_i \mathbf{U} = -\mathbf{U}_W \mathbf{U}_W^{-1} \tilde{\mathbf{A}} \mathbf{U}_W \mathbf{U}_W^{-1} \Delta_i \mathbf{U} = -\mathbf{U}_W \tilde{\mathcal{A}} \Delta_i \mathbf{W} = \mathbf{U}_W \breve{\phi}_{\mathsf{E}} \tag{85}$$

where $\breve{\phi}_{\mathsf{E}}$ is the fluctuation as computed for the auxiliary variables,

$$\breve{\phi}_{\mathsf{E}} = -\tilde{\mathcal{A}} \Delta_i \mathbf{W} \tag{86}$$

The flux Jacobian of the auxiliary variable formulation is obtained from the conserved flux Jacobian via the similarity transformation,

$$\tilde{\mathcal{A}} = \mathbf{U}_W^{-1} \tilde{\mathbf{A}} \mathbf{U}_W = \mathbf{U}_W^{-1} \tilde{\mathbf{X}} \tilde{\mathbf{\Lambda}} \tilde{\mathbf{X}}^{-1} \mathbf{U}_W = \tilde{\mathcal{X}} \tilde{\mathbf{\Lambda}} \tilde{\mathcal{X}}^{-1} \tag{87}$$

so the eigenvalue matrix, $\mathbf{\Lambda}$ (Eqn. 67), remains unaltered. The right eigenvectors are obtained from Eqns. 68 and 84,

$$\mathcal{X} = \mathbf{U}_W^{-1} \mathbf{X}$$

$$\mathcal{X}^{(1)} = \left\{ \begin{array}{c} 1 \\ 0 \\ 0 \end{array} \right\} \quad \mathcal{X}^{(2)} = \left\{ \begin{array}{c} 0 \\ a \\ a^2 \end{array} \right\} \quad \mathcal{X}^{(3)} = \left\{ \begin{array}{c} 0 \\ -a \\ a^2 \end{array} \right\} \tag{88}$$

The inverse is easily computed to be,

$$\mathcal{X}^{-1} = \left[\begin{array}{ccc} 1 & 0 & 0 \\ 0 & \frac{1}{2a} & \frac{1}{2a^2} \\ 0 & -\frac{1}{2a} & \frac{1}{2a^2} \end{array} \right] \tag{89}$$

The flux Jacobian is evaluated from Eqn. 87,

$$\tilde{A} = \begin{bmatrix} \tilde{u} & 0 & 0 \\ 0 & \tilde{u} & 1 \\ 0 & \tilde{a}^2 & \tilde{u} \end{bmatrix} \tag{90}$$

which corresponds to the following non-conservative form of the Euler equations,

$$\begin{aligned} s_t + us_x &= 0 \\ \rho u_t + u\rho u_x + P_x &= 0 \\ P_t + a^2\rho u_x + uP_x &= 0 \end{aligned} \tag{91}$$

Having developed an alternative method for obtaining the elemental fluctuation (Eqn. 85), the artificial dissipation can be addressed (Eqn. 78).

$$\phi'_{\mathsf{E}} = \text{sign}(\tilde{\mathbf{A}})\phi_{\mathsf{E}} = \mathbf{U}_W\mathbf{U}_W^{-1}\text{sign}(\tilde{\mathbf{A}})\mathbf{U}_W\breve{\phi}_{\mathsf{E}} = \mathbf{U}_W\breve{\phi}'_{\mathsf{E}} \tag{92}$$

where,

$$\breve{\phi}'_{\mathsf{E}} = \mathbf{U}_W^{-1}\text{sign}(\tilde{\mathbf{A}})\mathbf{U}_W\breve{\phi}_{\mathsf{E}} = \text{sign}(\tilde{A})\breve{\phi}_{\mathsf{E}} \tag{93}$$

and with the aid of Eqns. 79 and 87,

$$\text{sign}(\tilde{A}) = \mathbf{U}_W^{-1}\text{sign}(\tilde{\mathbf{A}})\mathbf{U}_W = \mathbf{U}_W^{-1}\tilde{\mathbf{X}}|\tilde{\mathbf{\Lambda}}|\tilde{\mathbf{\Lambda}}^{-1}\tilde{\mathbf{X}}^{-1}\mathbf{U}_W = \tilde{\mathcal{X}}|\tilde{\mathbf{\Lambda}}|\tilde{\mathbf{\Lambda}}^{-1}\tilde{\mathcal{X}}^{-1} \tag{94}$$

Using the eigenvalue and eigenvector definitions (Eqns. 67, 88, and 89) $\text{sign}(\tilde{A})$ is evaluated to be,

$$\text{sign}(\tilde{A}) = \begin{bmatrix} \text{sign}(\tilde{u}) & 0 & 0 \\ 0 & \frac{1}{2}\left[\text{sign}(\tilde{u}+\tilde{a}) + \text{sign}(\tilde{u}-\tilde{a})\right] & \frac{1}{2\tilde{a}}\left[\text{sign}(\tilde{u}+\tilde{a}) - \text{sign}(\tilde{u}-\tilde{a})\right] \\ 0 & \frac{\tilde{a}}{2}\left[\text{sign}(\tilde{u}+\tilde{a}) - \text{sign}(\tilde{u}-\tilde{a})\right] & \frac{1}{2}\left[\text{sign}(\tilde{u}+\tilde{a}) + \text{sign}(\tilde{u}-\tilde{a})\right] \end{bmatrix} \tag{95}$$

By considering two cases, for subsonic and supersonic conditions, Eqn. 95 takes on simple forms,

$$\text{sign}(\tilde{A}) = \begin{cases} \mathbf{M}^{sup} & \text{if} \quad |\tilde{u}| > \tilde{a} \\ \mathbf{M}^{sub} & \text{if} \quad |\tilde{u}| < \tilde{a} \end{cases} \tag{96}$$

where,

$$\mathbf{M}^{sup} = \text{sign}(\tilde{u})I \tag{97}$$

and,

$$\mathbf{M}^{sub} = \begin{bmatrix} \text{sign}(\tilde{u}) & 0 & 0 \\ 0 & 0 & \frac{1}{\tilde{a}} \\ 0 & \tilde{a} & 0 \end{bmatrix} \tag{98}$$

Navier-Stokes Equations

The Navier-Stokes equations[24, 25] for the flow of a perfect gas are written in one-dimensional conservation law form (Eqn. 58) with U defined in Eqn. 59 and the flux defined as,

$$\mathbf{F} = \mathbf{F}^i - \mathbf{F}^v \tag{99}$$

where the inviscid flux, $\mathbf{F}^i$, is the same as the Euler flux (Eqn. 60). The viscous flux is,

$$\mathbf{F}^v = \left\{ \begin{array}{c} 0 \\ \tau_{xx} \\ u\tau_{xx} - q_x \end{array} \right\} \tag{100}$$

Using Stokes' hypothesis the stress is,

$$\tau_{xx} = \frac{4}{3}\mu u_x \tag{101}$$

Fourier's law for heat flow gives,

$$q_x = -\kappa T_x \tag{102}$$

The thermal conductivity is related to the viscosity through the Prandtl number,

$$P_r = \frac{\mu c_p}{\kappa} \tag{103}$$

where for air $P_r = 0.72$[26]. The temperature is obtained from the perfect gas equation of state,

$$T = \frac{P}{\rho \Re} \tag{104}$$

The inviscid flux is discretized as described in the Euler Equations subsection. The contributions from the viscous flux to the nodal update is obtained in a Galerkin sense using the system analog to Eqn. 55. No viscous contribution is made to the continuity equation.

Using the linear variation of the parameter vector over an element, the velocity gradient is locally defined on an element[23, 27],

$$(u_x)_{\mathsf{E}} = \overline{\left(\frac{z_2}{z_1}\right)_x} = \overline{\frac{z_{2_x}}{z_1} - \frac{z_2}{z_1^2} z_{1_x}} = \frac{1}{\tilde{z}_1}\left(\Delta_i z_2 - \tilde{u}\Delta_i z_1\right) = \frac{\tilde{\rho}}{\tilde{z}_1^2}\Delta_i u = \frac{\tilde{\rho}}{\tilde{\tilde{\rho}}}\Delta_i u \tag{105}$$

where,

$$\tilde{\tilde{\rho}} = \tilde{z}_1^2 = \left(\frac{\sqrt{\rho_i} + \sqrt{\rho_{i+1}}}{2}\right)^2 \tag{106}$$

is called the consistent density average. The viscous contribution to the momentum equation can now be expressed,

$$\int_{\mathsf{E}} \frac{4}{3} v_x \mu u_x \, d\Omega = \frac{4}{3} v_x \bar{\mu} \frac{\tilde{\rho}}{\tilde{\tilde{\rho}}} \Delta_i u \tag{107}$$

The first term of the viscous energy flux is evaluated in a similar manner,

$$\int_{\mathsf{E}} \frac{4}{3} v_x \mu u u_x \, d\Omega = \frac{4}{3} v_x \bar{\mu} \tilde{u} \frac{\tilde{\rho}}{\tilde{\tilde{\rho}}} \Delta_i u \tag{108}$$

The second term requires some manipulation. Begin by defining the temperature gradient over an element,

$$(T_x)_{\mathsf{E}} = \overline{\left(\frac{P}{\rho\Re}\right)_x} = \overline{\frac{P}{\rho\Re}\left(\frac{P_x}{P} - \frac{\rho_x}{\rho}\right)} = \frac{\tilde{a}^2}{\gamma\Re}\left(\frac{\Delta_i P}{\tilde{P}} - \frac{\Delta_i \rho}{\tilde{\rho}}\right) \tag{109}$$

where,

$$\tilde{P} = \frac{\tilde{a}^2\tilde{\rho}}{\gamma} \tag{110}$$

The heat flow contribution to the viscous flux is then obtained,

$$\int_{\mathsf{E}} v_x \kappa T_x \, d\Omega = v_x \bar{\kappa}\frac{\tilde{a}^2}{\gamma\Re}\left(\frac{\Delta_i P}{\tilde{P}} - \frac{\Delta_i \rho}{\tilde{\rho}}\right) = v_x \frac{\bar{\mu}c_p}{P_r}\frac{\tilde{a}^2}{\gamma\Re}\left(\frac{\Delta_i P}{\tilde{P}} - \frac{\Delta_i \rho}{\tilde{\rho}}\right) \tag{111}$$

The elemental contributions from the viscous terms is similar to Eqn. 56.

$$\begin{aligned} S_i \mathbf{U}_{i_t} &\leftarrow \frac{\bar{\mu}_{i+\frac{1}{2}}}{\ell_{i,i+1}} \left\{ \begin{array}{c} 0 \\ \frac{4}{3}\frac{\tilde{\rho}}{\tilde{\rho}}\Delta_i u \\ \frac{4}{3}\tilde{u}\frac{\tilde{\rho}}{\tilde{\rho}}\Delta_i u + \frac{c_p}{P_r}\frac{\tilde{a}^2}{\gamma\Re}\left(\frac{\Delta_i P}{P} - \frac{\Delta_i \rho}{\tilde{\rho}}\right) \end{array} \right\} + \text{COE} \\ S_{i+1} \mathbf{U}_{i+1_t} &\leftarrow -\frac{\bar{\mu}_{i+\frac{1}{2}}}{\ell_{i,i+1}} \left\{ \begin{array}{c} 0 \\ \frac{4}{3}\frac{\tilde{\rho}}{\tilde{\rho}}\Delta_i u \\ \frac{4}{3}\tilde{u}\frac{\tilde{\rho}}{\tilde{\rho}}\Delta_i u + \frac{c_p}{P_r}\frac{\tilde{a}^2}{\gamma\Re}\left(\frac{\Delta_i P}{P} - \frac{\Delta_i \rho}{\tilde{\rho}}\right) \end{array} \right\} + \text{COE} \end{aligned} \tag{112}$$

As discussed for the scalar advection/diffusion equations, when solving the Navier-Stokes equations the maximum of the viscous contribution to the nodal update and the artificial dissipation from the inviscid flux discretization should be utilized. When the physical viscous terms are large enough, no artificial dissipation is needed.

Summary

The equivalence of the discretized equations using both the fluctuation splitting and finite volume approaches has been shown for non-uniform one-dimensional domains. Advection and diffusion, both separately and together, have been considered for scalar equations. For systems, the equivalence of the Roe flux-difference-split finite volume scheme and Sidilkover's fluctuation splitting scheme for Euler equations is shown. Finally, viscous diffusion and conduction terms are modeled and included, establishing the equivalence for the discretized Navier-Stokes equations. The strong link established in one dimension can serve as a prelude to multidimensional analysis of fluctuation splitting and finite volume as applied to viscous gas dynamics.

Appendix—Limiters

A limiter is a function designed to limit the ratio of two values, satisfying,

$$\psi(0) = 0, \quad \psi(1) = 1 \tag{113}$$

A symmetric limiter is defined by,

$$\psi\left(\frac{p}{q}\right) = \frac{p}{q}\,\psi\left(\frac{q}{p}\right) \tag{114}$$

Symmetric limiters can also be expressed in terms of symmetric averaging functions, M_ψ, obeying,

$$q\,\psi\left(\frac{p}{q}\right) = M_\psi(p,q) = M_\psi(q,p) = p\,\psi\left(\frac{q}{p}\right) \tag{115}$$

A limiter that can achieve a value greater than unity is termed a compressive limiter.

First Order

The first order limiter, so called because it is usually employed to limit a scheme to first order spatial accuracy, is the trivial limiter,

$$\psi = M_\psi = 0 \tag{116}$$

Minmod

The minmod limiter[4] is a non-compressive, symmetric limiter defined as,

$$\psi\left(\frac{p}{q}\right) = \max(0,\ \min(1,\ p/q)) \tag{117}$$

or,

$$\psi\left(\frac{p}{q}\right) = \begin{cases} 0 & pq \le 0 \\ p/q & \text{if} \quad |p| \le |q| \\ 1 & |p| \ge |q| \end{cases} \tag{118}$$

The associated averaging function is,

$$M_\psi(p,q) = \begin{cases} 0 & pq \le 0 \\ p & \text{if} \quad |p| \le |q| \\ q & |p| \ge |q| \end{cases} \tag{119}$$

The minmod limiter is the non-compressive limit of a generalized β limiter of Sweby[28]. Minmod is achieved by $\beta = 1$. The upper limit on β is the "superbee" limiter, $\beta = 2$.

$$\psi\left(\frac{p}{q}\right) = \max[0,\ \min(\beta p/q,\ 1),\ \min(p/q,\ \beta)] \tag{120}$$

$$\psi\left(\frac{p}{q}\right) = \begin{cases} 0 & pq \le 0 \\ \beta p/q & \beta|p| \le |q| \\ 1 \quad \text{if} & |p| \le |q| \le \beta|p| \\ p/q & |q| \le |p| \le \beta|q| \\ \beta & \beta|q| \le |p| \end{cases} \tag{121}$$

$$M(p,q) = \begin{cases} 0 & pq \le 0 \\ \beta p & \beta|p| \le |q| \\ q \quad \text{if} & |p| \le |q| \le \beta|p| \\ p & |q| \le |p| \le \beta|q| \\ \beta q & \beta|q| \le |p| \end{cases} \tag{122}$$

A similar, non-symmetric limiter has been proposed by Chakravarthy[29],

$$\psi\left(\frac{p}{q}\right) = \max[0,\ \min(p/q,\ \beta)] \tag{123}$$

$$\psi\left(\frac{p}{q}\right) = \begin{cases} 0 & pq \le 0 \\ p/q \quad \text{if} & |p| \le \beta|q| \\ \beta & |p| \ge \beta|q| \end{cases} \tag{124}$$

The upper bound on this limiter is $1 \le \beta \le 2$.

van Leer

The van Leer limiter[30] is a symmetric compressive limiter with an upper bound of 2.

$$\psi\left(\frac{p}{q}\right) = \frac{\frac{p}{q} + \left|\frac{p}{q}\right|}{1 + \frac{p}{q}} = \frac{pq + |pq|}{q^2 + pq} \tag{125}$$

$$M_\psi = \frac{pq + |pq|}{q + p} \tag{126}$$

van Albada

The van Albada limiter[31] is a symmetric compressive limiter with an upper bound of 1.18.

$$\psi\left(\frac{p}{q}\right) = \frac{\left(\frac{p}{q}\right)^2 + \frac{p}{q}}{1 + \left(\frac{p}{q}\right)^2} = \frac{p(p+q)}{p^2 + q^2}, \quad pq > 0, \quad \text{zero otherwise} \tag{127}$$

$$M_\psi = \frac{pq(p+q)}{p^2 + q^2}, \quad pq > 0 \tag{128}$$

References

[1] Roe, P. L., "Approximate Riemann Solvers, Parameter Vectors, and Difference Schemes," *Journal of Computational Physics*, Vol. 43, October 1981, pp. 357–372.

[2] Roe, P. L., "Characteristic-Based Schemes for the Euler Equations," *Annual Review of Fluid Mechanics*, Vol. 18, 1986, pp. 337–365.

[3] van Leer, B., "Towards the Ultimate Conservative Scheme. V. A Second-Order Sequel to Godunov's Method," *Journal of Computational Physics*, Vol. 32, 1979, pp. 101–136.

[4] Hirsch, C., *Numerical Computation of Internal and External Flows—Volume 2: Computational Methods for Inviscid and Viscous Flows*, John Wiley & Sons Ltd., 1990.

[5] Barth, T. J., "Aspects of Unstructured Grids and Finite-Volume Solvers for the Euler and Navier-Stokes Equations," *Computational Fluid Dynamics*, No. 1994–04 in Lecture Series, von Karman Institute for Fluid Dynamics, 1994.

[6] Deconinck, H., Struijs, R., and Roe, P. L., "Fluctuation Splitting for Multidimensional Convection Problems: An Alternative to Finite Volume and Finite Element Methods," *Computational Fluid Dynamics*, No. 1990–03 in Lecture Series, von Karman Institute for Fluid Dynamics, Mar. 1990.

[7] Hirsch, C., "A General Analysis of Two-Dimensional Convection Schemes," *Computational Fluid Dynamics*, Lecture Series 1991-01, von Karman Institute for Fluid Dynamics, Feb. 1991.

[8] Deconinck, H., Struijs, R., Bourgois, G., and Roe, P. L., "Compact Advection Schemes on Unstructured Grids," *Computational Fluid Dynamics*, No. 1993–04 in Lecture Series, von Karman Institute for Fluid Dynamics, Mar. 1993.

[9] Sidilkover, D., "A Genuinely Multidimensional Upwind Scheme and Efficient Multigrid Solver for the Compressible Euler Equations," Report 94–84, ICASE, USA, Nov. 1994.

[10] Sidilkover, D., "Multidimensional Upwinding and Multigrid," AIAA Paper 95–1759, Jun. 1995.

[11] Sidilkover, D. and Roe, P. L., "Unification of Some Advection Schemes in Two Dimensions," Report 95–10, ICASE, Hampton, Feb. 1995.

[12] Sidilkover, D., "Some Approaches Towards Constructing Optimally Efficient Multigrid Solvers for the Inviscid Flow Equations," Report 97–39, ICASE, Hampton, Aug. 1997.

[13] Deconinck, H., Paillère, H., Struijs, R., and Roe, P. L., "Multidimensional Upwind Schemes Based on Fluctuation-Splitting for Systems of Conservation Laws," *Computational Mechanics*, Vol. 11, 1993, pp. 323–340.

[14] Godunov, S. K., "A Difference Method for the Numerical Calculation of Discontinuous Solutions of Hydrodynamic Equations," *Matematichaskiy Sbornik*, Vol. 47(89), No. 3, Mar. 1959, pp. 271–306.

[15] Courant, R., Isaacson, E., and Reeves, M., "On the Solution of Nonlinear Hyperbolic Differential Equations by Finite Differences," *Pure and Applied Mathematics*, Vol. 5, 1952, pp. 243–255.

[16] Harten, A. and Hyman, J. M., "Self Adjusting Grid Methods for One-Dimensional Hyperbolic Conservation Laws," *Journal of Computational Physics*, Vol. 50, 1983, pp. 235–269.

[17] Anderson, W. K. and Bonhaus, D. L., "An Implicit Upwind Algorithm for Computing Turbulent Flows on Unstructured Grids," *Computers and Fluids*, Vol. 23, No. 1, Jan. 1994, pp. 1–21.

[18] Tomaich, G. T., *A Genuinely Multi-Dimensional Upwinding Algorithm for the Navier-Stokes Equations on Unstructured Grids Using a Compact, Highly-Parallelizable Spatial Discretization*, Ph.D. thesis, University of Michigan, USA, 1995.

[19] Bickford, W. B., *A First Course in the Finite Element Method*, Richard D. Irwin, Inc., Boston, 1990.

[20] Bathe, K.-J., *Finite Element Procedures in Engineering Analysis*, Prentice-Hall, Inc., Englewood Cliffs, USA, 1982.

[21] Barth, T. J., "Recent Developments in High Order K-Exact Reconstruction on Unstructured Meshes," AIAA Paper 93–0668, Jan. 1993.

[22] Euler, L., "Principes Généraux du Mouvement des Fluides," *Historical Academy of Berlin, Opera Omnia II*, Vol. 12, 1755, pp. 54–92.

[23] Deconinck, H., Roe, P. L., and Struijs, R., "A Multidimensional Generalization of Roe's Flux Difference Splitter for the Euler Equations," *Computers and Fluids*, Vol. 22, No. 2/3, 1993, pp. 215 222.

[24] Navier, M., "Mémoire sur les lois du Mouvement des Fluides," *Mémoire de l'Académie des Sciences*, Vol. 6, 1827, pp. 389.

[25] Stokes, G. G., "On the Theories of the Internal Friction of Fluids in Motion," *Trans. Cambridge Philosophical Society*, Vol. 8, 1849, pp. 227 319.

[26] Anderson, D. A., Tannehill, J. C., and Pletcher, R. H., *Computational Fluid Mechanics and Heat Transfer*, Taylor and Francis, 1984.

[27] Struijs, R., Deconinck, H., de Palma, P., Roe, P., and Powell, K. G., "Progress on Multidimensional Upwind Euler Solvers for Unstructured Grids," AIAA Paper 91–1550, Jun. 1991.

[28] Sweby, P. K., "High Resolution Schemes Using Flux Limiters for Hyperbolic Conservation Laws," *SIAM Journal of Numerical Analysis*, Vol. 21, 1984, pp. 995–1011.

[29] Chakravarthy, S. R. and Osher, S., "High Resolution Applications of the Osher Upwind Scheme for the Euler Equations," AIAA Paper 83–1943, Jun. 1983.

[30] van Leer, B., "Towards the Ultimate Conservative Scheme. II. Monotonicity and Conservation Combined in a Second Order Scheme," *Journal of Computational Physics*, Vol. 14, 1974, pp. 361–370.

[31] van Albada, G. D., van Leer, B., and Roberts, W. W., "A Comparative Study of Computational Methods in Cosmic Gas Dynamics," Report 81–24, ICASE, NASA Langley Research Center, Hampton, Virginia, August 1981.

REPORT DOCUMENTATION PAGE

Form Approved
OMB No. 0704–0188

1. AGENCY USE ONLY *(Leave blank)*	2. REPORT DATE	3. REPORT TYPE AND DATES COVERED
	October 1997	Technical Memorandum

4. TITLE AND SUBTITLE
Equivalence of Fluctuation Splitting and Finite Volume for One-Dimensional Gas Dynamics

5. FUNDING NUMBERS
WU 242-80-01-01

6. AUTHOR(S)
William A. Wood

7. PERFORMING ORGANIZATION NAME(S) AND ADDRESS(ES)
NASA Langley Research Center
Hampton, VA 23681–2199

8. PERFORMING ORGANIZATION REPORT NUMBER
L–17677

9. SPONSORING/MONITORING AGENCY NAME(S) AND ADDRESS(ES)
National Aeronautics and Space Administration
Washington, DC 20546–0001

10. SPONSORING/MONITORING AGENCY REPORT NUMBER
NASA/TM–97–206271

11. SUPPLEMENTARY NOTES

12a. DISTRIBUTION/AVAILABILITY STATEMENT
Unclassified-Unlimited
Subject Category 64 Distribution: Nonstandard
Availability: NASA CASI (301) 621–0390

12b. DISTRIBUTION CODE

13. ABSTRACT ***(Maximum 200 words)***

The equivalence of the discretized equations resulting from both fluctuation splitting and finite volume schemes is demonstrated in one dimension. Scalar equations are considered for advection, diffusion, and combined advection/diffusion. Analysis of systems is performed for the Euler and Navier-Stokes equations of gas dynamics. Non-uniform mesh-point distributions are included in the analyses.

14. SUBJECT TERMS
CFD, Fluctuation Splitting

15. NUMBER OF PAGES
29

16. PRICE CODE
A03

17. SECURITY CLASSIFICATION OF REPORT	18. SECURITY CLASSIFICATION OF THIS PAGE	19. SECURITY CLASSIFICATION OF ABSTRACT	20. LIMITATION OF ABSTRACT
Unclassified	Unclassified	Unclassified	